Detectability of exomoons by examining the signals from a model of transiting exoplanets with moons

P Cherdwongsung[1*], S Awiphan[2†], P Kittara[3‡], K Matan[3] and N Nakharutai[4]

[1]Master's Degree Program in Physics, Department of Physics, Faculty of Science, Mahidol University, Bangkok, 10400, Thailand
[2]National Astronomical Research Institute of Thailand (Public Organization), Chiang Mai, 50180, Thailand
[3]Department of Physics, Faculty of Science, Mahidol University, Bangkok, 10400, Thailand
[4]Department of Statistics, Faculty of Science, Chiang Mai University, Chiang Mai, 50200, Thailand

E-mail: *prangsutip.chr@student.mahidol.ac.th, †supachai@narit.or.th, ‡phichet.kit@mahidol.ac.th

Abstract. Exomoons are natural satellites of exoplanets. Nowadays, none has been confirmed. However, a number of detection techniques have been proposed, including Transit Timing Variations (TTV) and Transit Duration Variations (TDV) techniques. From a recent study, fitting observed transit with the traditional photocentric fitting model shows unique features around the primary and secondary exomoon transits in TDV and transit depth signals, which might reduce the detectability. The aim of this work is to retrieve the variation of TTV, TDV and transit depth signals of exomoon systems with the photocentric fitting model. One year star-planet-moon transit light curves are simulated with `LUNA` algorithm and fit with `TransitFit`. The results show that neglecting the TDV and transit depth data with phase around exomoon's primary and secondary transits improve the exomoon detectability by a factor of ten and the systems with large moon orbital semi-major axis with nearly edge-on orbit around low mass stars can be detected.

1. Introduction

In the Solar system, more than 200 moons have been discovered. However, to date, none of moon orbiting exoplanet, an exomoon, has been discovered. Only two exomoon candidates: MOA-2011-BLG-262Lb [1] and Kepler-1625 b I [2], have been proposed. A number of exomoon detection techniques have been proposed, including the transit [3], microlensing [4], transit timing variation [5, 6] and transit duration variation [7] techniques.

The transit method is one of the most promising methods for searching exoplanets. More than 2,000 exoplanets have been discovered with the technique. The shape of transit light curves provides physical information of the exoplanetary system, including the mid-transit time and transit duration. In a planetary system with a satellite, the gravitation interactions of an exomoon can alter the exoplanet's transit time, called transit timing variation (TTV) effect. Moreover, the transverse velocity of the planet also varies with the moon position which causes the change in transit duration, called transit duration variation effects. The root mean square amplitude of TTV and TDV sinusoidal signal can be written as,

$$\delta_{TTV} \simeq \frac{1}{\sqrt{2}} \frac{a_m M_m \sqrt{a_p}}{(M_p + M_m)\sqrt{G(M_s + M_p + M_m)}} \ , \tag{1}$$

and

$$\delta_{TDV} \simeq \left[\frac{a_w a_p \cos^2 i}{(R_s + R_p)^2 - a_p^2 \cos^2 i} \pm \frac{2\pi a_w}{P_m} \frac{1}{v_{B\perp}} \right] \cdot \frac{\overline{\tau}}{\sqrt{2}} \ , \tag{2}$$

respectively, where a_m and a_w are the semi-major axes moon's and planet's orbit around the planet-moon barycentre, respectively, a_p is the planet orbital semi-major axis, M_s is the stellar mass, M_p is the planetary mass, M_m is the moon mass, i is the orbital inclination angle of both planet and moon orbits with the coplanar orbit is assumed, R_s is the star radius, R_p is the planet radius, $v_{B\perp}$ is the projected velocity of the planet-moon barycentre across the face of the star during transit, P_m is the moon orbital period, $\overline{\tau}$ is the transit duration, and G is the universal gravitational constant. Therefore, the TTV and TDV signals depend on eight parameters: M_s, M_p, M_m, R_s, R_p, a_p, a_m and i.

However, fitting transiting exoplanet with moon light curves using the photocentric fitting model, the TTV, TDV and transit depth signals are perturbed due to exomoon transits at the moon phase $\phi_m = 0.25, 0.75$ or around the phases when the moon transits inside the planetary disc at primary exomoon transit and secondary exomoon transit. The exomoon transit induces larger variation in TDV and transit depth signals than the TTV signal (figure 1).

In this paper, the TDV and transit depth perturbations effects at the primary and secondary moon's transits on the detectabilities are investigated. The transiting exoplanet with exomoon light curves are simulated using `LUNA` algorithm [8]. The light curves are fitted with `TransitFit`, which is a photocentric fitting model [9]. The moon phases are computed from the cyclic variation of TTV signals. The sinusoidal variation of the TDV and transit depth data with cutting and non-cutting the moon phases around the moon's transit models are compared.

2. Generating transiting exoplanet with moon light curves

The transiting exoplanet with exomoon light curves were generated by `LUNA` algorithm [8]. One year light curves are simulated. The number of light curves depend on their planetary orbital period. The orbital periods are set to be less than 18 days in order to have the number of transits large enough (> 20 transits) to perform the statistic test. In each light curve, 20,000 data points are simulated throughout the orbital period.

A Neptune-mass exomoon orbiting a Jupiter-mass exoplanet is focused in this work. The moon's massses and radii are followed mass-radius relationship of Neptune-mass exoplanet [10]. The moon radii are limited to be four times smaller than their planetary host radii. The planet-moon separations are constrained mainly by the Hill's stability. The moon periods that are orbital resonance with their host planets orbital period are neglected. The moons are orbiting in the same orbital plane of their host planet orbit ($i_m = i_p$). The systems whose the moon do not transit the host star ($b_m > 1$) is neglected. Both planets and their satellites are assume to have circular orbital ($e_p = 0$ and $e_m = 0$). The host stars are main sequence stars followed mass-radius relation by Eker Z *et al* [11] with TESS limb darkening coefficients [12]. The TESS bandpass covers the wavelength from 600 - 1,000 nm and is centered on the traditional Cousins I-band. The summarized of simulated systems is shown in table 1.

3. Generating TTV, TDV and transit depth signals

The simulated light curves are fitted with `TransitFit` package [9]. The simulated light curves are shorten to 1,000 data points for transit event. First of all, all simulated light curves are fitted in order to obtain the planetary orbital period and inclination of the systems. The period and

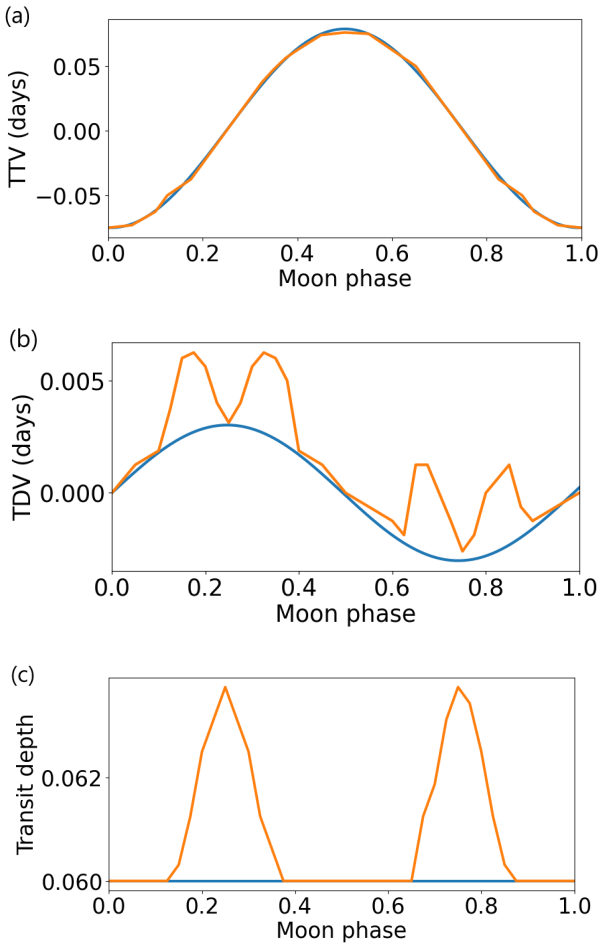

Figure 1. The theoretical moon phase evolution of TTVs (a), TDVs (b) and transit depth (c) signals (Blue) with photocentric fitting model (Orange). The model TDV and transit depth signal show a large variation around exomoon's transit phases.

inclination from the fitting are set to be fixed value for the second fitting where each transit is fitted individually (figure 2). In the second fitting, mid-transit time (t_0), planetary semi-major axis (a_p/R_*), planet-star radius ratio (R_p/R_s) and limb darkening coefficients of each transit are obtained. The TTV, TDV and transit depth are calculated from fitted mid-transit times, planetary semi-major axes and planet-star radius ratios, respectively.

4. TTV, TDV and transit depth analyses

Since the TTV signal is less affected from the perturbing of moon transit as shown in figure 1, the moon periods are derived from the highest peak of TTV's periodgram obtained from Lomb-Scargle periodogram package [13]. The systems with moon periods that have false alarm probability < 0.1 is selected. Only 83% of the simulated systems pass this criterion. The obtained period is used to calculate the moon phase. An example of phase-folded of TTV signal is shown in figure 3.

The example of phase-folded of TDV and transit depth signals are shown in figure 4 and 5. The signals are fitted with sine function. The goodness of fitting is defined by the chi-square value, χ^2. However, both TDV and transit depth signals show anomalies signals around primary

Table 1. The input parameters for generating Neptune-mass exomoon orbiting a Jupiter-mass exomoon around main sequence stars light curves with `LUNA` algorithm.

Parameters		**Value**			
Planetary mass	(M_p)	150.0	-	5000.0	$M_\oplus$
Planetary radius	(R_p)	12.225	-	14.264	$R_\oplus$
Moon mass	(M_m)	10.0	-	50.0	$M_\oplus$
Moon radius	(R_m)	3.137	-	3.560	$R_\oplus$
Planetary semi-major axis	(a_p)	0.1	-	1.0	AU
Moon semi-major axis	(a_m)	0.00857	-	0.193	AU
Planet inclination	(i_p)	78.707	-	90.0	degree
Stellar mass	(M_s)	0.179	-	2.80	$M_\odot$
Stellar radius	(R_s)	0.175	-	4.209	$R_\odot$

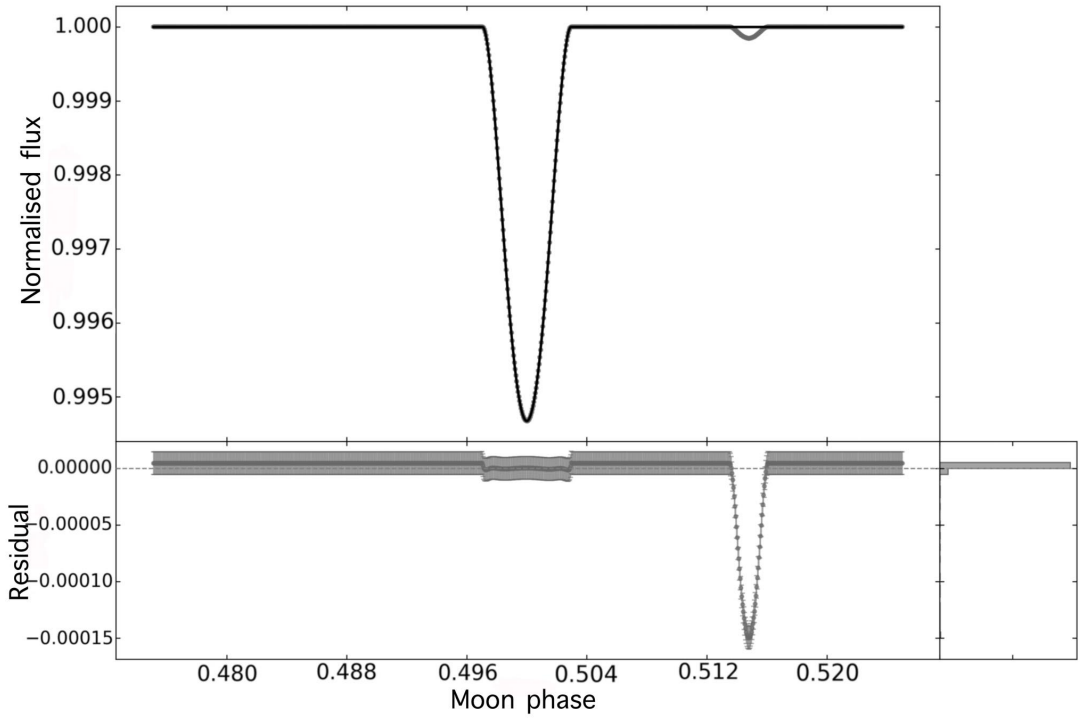

Figure 2. The star-planet-moon transit light curve with best-fit transit model (top) and its residuals from `TransitFit`. The bigger dip shows a planet transit and the smaller dip show a moon transit.

exomoon transit ($\phi_m = 0.15 - 0.35$) and secondary exomoon transit ($\phi_m = 0.65 - 0.85$) as discussed in section 1. Therefore, the phases around these transits are cut. The cut signals are also fitted with sine function (figure 4 and 5).

The theoretical model of TDV signals are sinusoidal functions with the same period and phase shift of $\pi/2$ of TTV sinusoidal function [7]. Neglecting exomoon transit, the transit depths are constant. For non-cutting moon phase model, the number of system with the reduced χ^2 are less than critical values at 99% significance level are 1% and 6% for TDV and transit depth

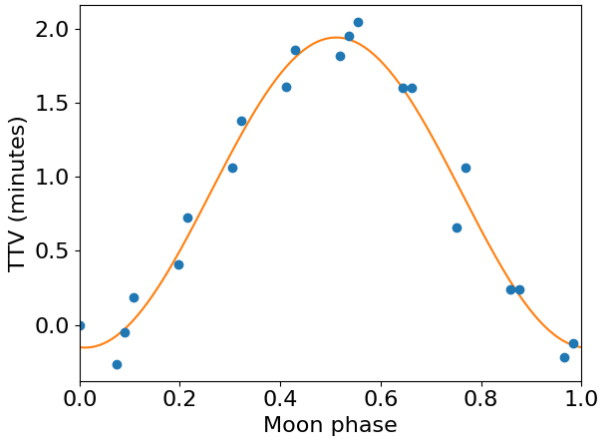

Figure 3. The phase-folded TTV signals from `TransitFit` (Blue dot) with its sinusoidal model (Orange line).

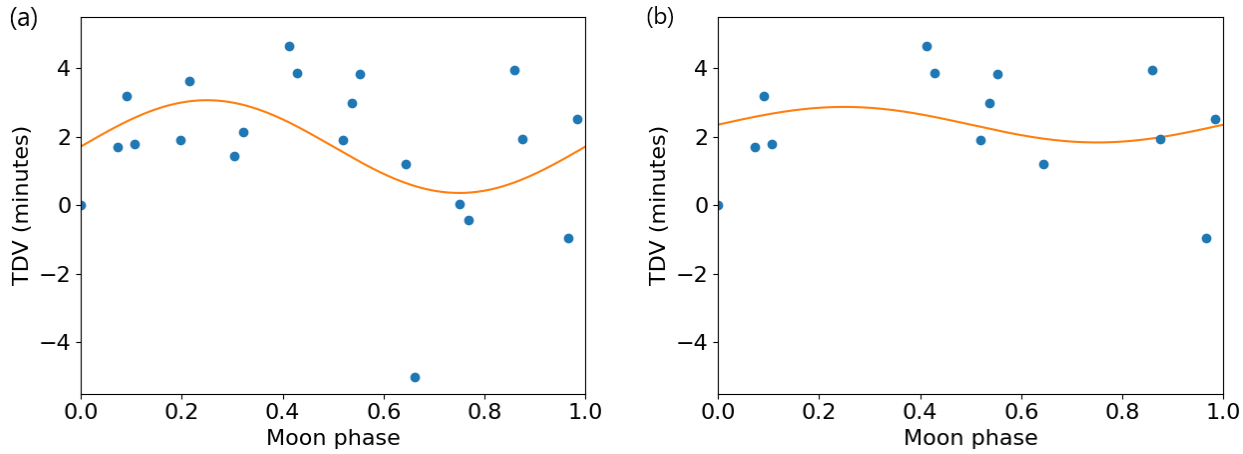

Figure 4. The phase-folded TDV signals from `TransitFit` (Blue dot) with its sinusoidal model (Orange line) of non-cuting moon phase model (a) and cutting moon phase model (b). The reduced χ^2 values of the models are 3.01 and 2.15, respectively.

data, respectively. However, for the cutting moon phase model, the number of system with the reduced χ^2 are less than critical values at 99% significance level increase to 11% and 85% for TDV and transit depth, respectively (figure 6). Therefore, cutting moon phase around exomoon transits can improve the exomoon detectability by a factor of ten.

As the number of systems which pass the TDV critical values is less than those with transit depth critical values. Only the systems which pass the TDV critical values are focused. The distribution between four parameters: moon orbital semi-major axis, planet inclination, stellar radius and stellar mass, with their reduced chi-square values are shown in figure 7. The systems with large moon orbital radius (> 0.01 AU) and high inclination ($> 87°$) around low mass stars can be detected in this work.

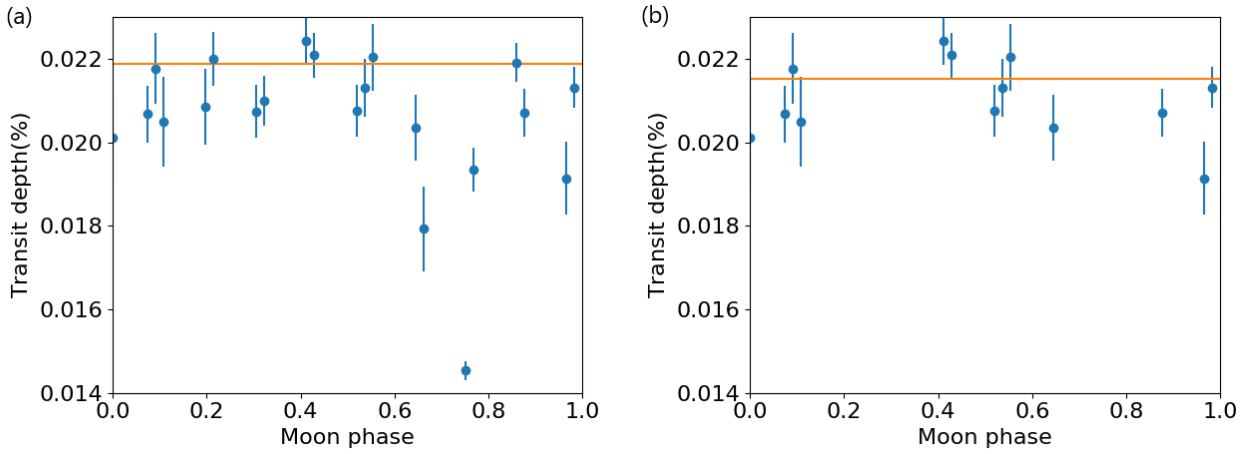

Figure 5. The phase-folded transit depth signals from `TransitFit` (Blue dot) with a constant transit depth value (Orange line) of non-cuting moon phase model (a) and cutting moon phase model (b). The reduced χ^2 values of the models are 68.8 and 2.15, respectively.

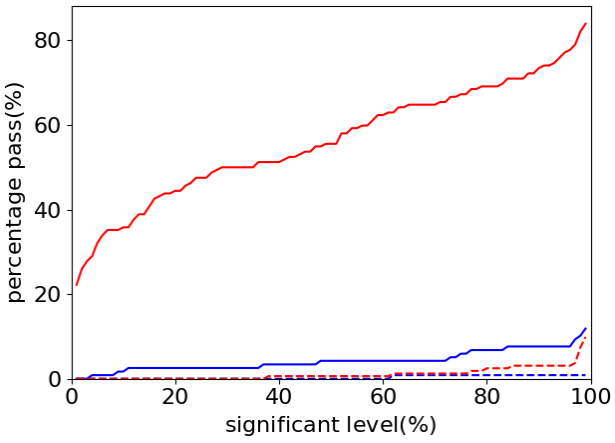

Figure 6. The significant level and the number of system which below their critical value of TDV (Blue) and transit depth (Red) data with non-cutting moon phase (Dashed line) and cutting moon phase (Solid line) models.

5. Conclusions

Neptune-mass exomoon orbiting a Jupiter-mass exomoon around main sequence stars light curves are simulated. Searching exomoon with TTV and TDV techniques using the photocentric fitting model can improve the the exomoon detectabilities by cutting the TDV and transit depth data around primary and secondary moon transits. The TDV still be the weakest signals to detect with photocentric fitting model. Only the systems with large moon orbital radius (> 0.01 AU) with nearly edge-on orbit ($> 87°$) around low mass stars can be detected.

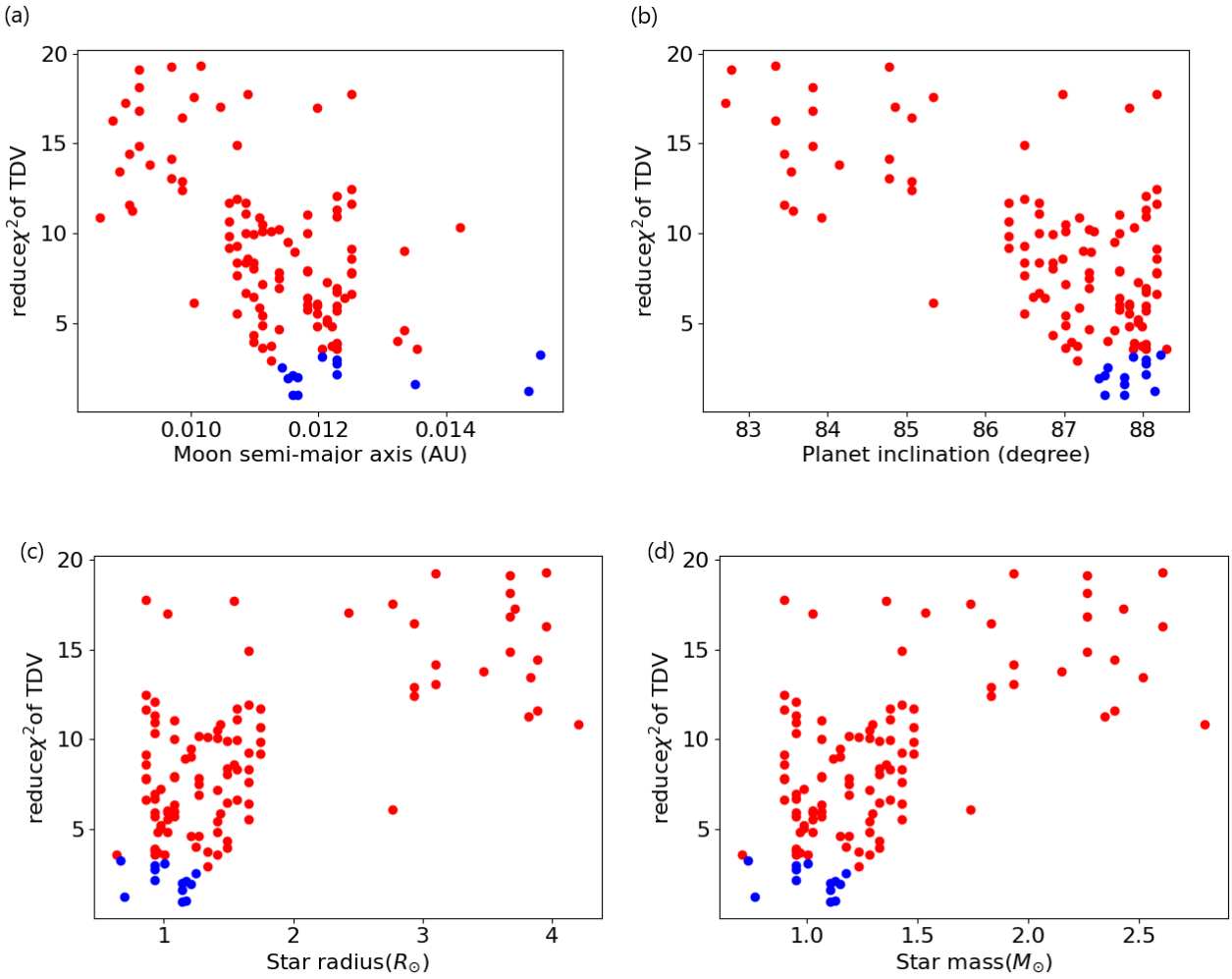

Figure 7. The relations between four physical parameters: moon orbital semi major axis (a), planet inclination (b), star radius (c) and star mass (d), and reduced χ^2 of TDV data below (Blue) and above (Red) the critical values at 99% significance level.

Acknowledgment

We acknowledge the financial support from National Astronomical Research Institute of Thailand (NARIT). SA acknowledge the financial support from a research funding project for young scientist researchers, The Coordinating Center for Thai Government Science and Technology Scholarship Students, National Science and Technology Development Agency.

References

[1] Bennett D P *et al* 2014 MOA-2011-BLG-262Lb: A sub-earth-mass moon orbiting a gas giant primary or a high velocity planetary system in the galactic bulge *Astrophys. J.* **785** 155

[2] Teachey A and Kipping D M 2018 Evidence for a large exomoon orbiting Kepler-1625b *Sci. Adv.* **4** eaav1784

[3] Simon A, Szatmary K and Szabo G M 2007 Determination of the size, mass, and density of "exomoons" from photometric transit timing variations *Astron. Astrophys.* **470** 727–31

[4] Han C and Han W 2002 On the feasibility of detecting satellites of extrasolar planets via microlensing *Astrophys. J.* **580** 490–93
[5] Sartoretti P and Schneider J 1999 On the detection of satellites of extrasolar planets with the method of transits *Astron. Astrophys. Suppl. Ser.* **134** 553–60
[6] Kipping D M 2008 Transit timing effects due to an exomoon *Mon. Notices Royal Astron. Soc.* **392** 181–9
[7] Kipping D M 2009 Transit timing effects due to an exomoon - II *Mon. Notices Royal Astron. Soc.* **396** 1797–804
[8] Kipping D M 2011 LUNA: an algorithm for generating dynamic planet-moon transits *Mon. Notices Royal Astron. Soc.* **416** 689–709
[9] Hayes J J C *et al* 2021 TransitFit: an exoplanet transit fitting package for multi-telescope data sets and its application to WASP-127, WASP-91, and WASP-126 *ArXiv* 2103.12139
[10] Chen J and Kipping D M 2016 Probabilistic forecasting of the masses and radii of other world *Astrophys. J.* **834** 17
[11] Eker Z *et al* 2018 Interrelated main-sequence mass–luminosity, mass–radius, and mass–effective temperature relations *Mon. Notices Royal Astron. Soc.* **479** 5491–511
[12] Claret A 2017 Limb and gravity-darkening coefficients for the TESS satellite at several metallicities, surface gravities, and microturbulent velocities *Astron. Astrophys.* **600** 6
[13] VanderPlas J T 2018 Understanding the Lomb-Scargle Periodogram *Astrophys. J. Suppl. Ser.* **236** 16